Journal of Constructional Steel Research 148 (2018) 189–197

Contents lists available at ScienceDirect

Journal of Constructional Steel Research

Stability of steel columns stiffened by stays and multiple crossarms

Pengcheng Li [a,b,*], Ce Liang [c], Jun Yuan [c], Ke Qiao [c]

[a] Key Laboratory of New Technology for Construction of Cities in Mountain Area (Chongqing University), Ministry of Education, Chongqing 400045, China
[b] School of Civil Engineering, Chongqing University, Chongqing 400045, China
[c] College of Engineering and Technology, Southwest University, Chongqing 400715, China

ARTICLE INFO

Article history:
Received 17 March 2018
Received in revised form 15 May 2018
Accepted 19 May 2018
Available online xxxx

Keywords:
PSSC
Buckling behaviour
Multi-crossarms
Post-buckling

ABSTRACT

A pre-stressed stayed steel column (PSSC) can effectively enhance the buckling behaviour of compression columns. In the past, researchers have primarily concentrated on examining the behaviour of PSSCs with single-bay crossarms. However, research focused on PSSCs with multiple crossarms is limited. This article aims to investigate the stability behaviour of PSSCs stiffened with multiple crossarms according to geometric analysis in conjunction with finite element (FE) studies. The results show that the critical buckling modes can be complicated due to the introduction of multiple crossarms. Critical buckling deformation similar to three half sine waves can be observed. It has also been demonstrated that interactive buckling can be ignored when determining the actual buckling strength of PSSCs stiffened by multiple crossarms, though it must be considered for PSSCs with single-bay crossarms. The effects of stay diameter and pretension in the stay have been separately investigated, and the results show that the buckling strength of a steel column can be obviously enhanced even if the pretension in stays is quite small, because the stiffness of the stays can be automatically activated by column deformation.

1. Introduction

Global buckling tends to occur in compressed steel columns when they are slender. However, the buckling resistance can be drastically improved by introducing stays and crossarms. The compressed steel column, which is equipped with stays and crossarms, has been named prestressed stayed steel columns (PSSC). In the PSSC shown in Fig. 1, an additional restraint can be placed on the main column by the crossarms in conjunction with pre-tensioned stays.

Research on PSSC has been conducted since the 1960s, in which Chu and Berge first investigated the critical buckling loads in PSSCs [1]. Following the work of Chu and Berge, Hafez quantitatively examined the effect of pretension on the buckling load by theoretical derivation based on the assumption of small deformations [2]. With the development of computer technology, particularly over the last twenty years, nonlinear buckling analysis in PSSCs by finite element (FE) software became possible. Thus, geometric imperfections governing nonlinear buckling [3–5], evaluate the post-buckling behaviour [6,7], and investigate the optimum design method can be conducted numerically [8,9]. Experimental studies have also been conducted in parallel with FE analyses on PSSCs [10–14].

For practical application of PSSCs, the compressed steel columns are generally stiffened by spatial crossarm systems (see Fig. 2) around the main column and multiple crossarms along the main column length (see Fig. 2(b)). Unfortunately, most of the previous studies concentrated on investigating PSSCs with crossarms only set at the mid-span of the main column (see Fig. 2(a)), which are not typically found in practice. As far as the authors are aware, references [15, 16] are the only studies aimed at investigating the stability of PSSCs with multiple crossarms. However, the interactive buckling behaviour of PSSCs with multiple crossarms has not been investigated. In fact, research on PSSCs with single-bay crossarms shows that interactive buckling may become dominant when determining the actual buckling strength.

Based on the background information introduced above, this current work focuses on investigating the stability of PSSCs stiffened with multiple crossarms along the main column length. First, pretension was derived by geometric analysis, which corresponds to the maximum critical buckling load. This pretension level was used as the benchmark pretension value in the FE simulation. Subsequently, critical and nonlinear buckling analyses were conducted to explore the buckling strength of PSSCs stiffened with multiple crossarms. In addition, a discussion based on parametric analysis results was presented to quantitatively examine the effect of cross-sectional area of the stays and pretension in stays.

* Corresponding author at: Key Laboratory of New Technology for Construction of Cities in Mountain Area (Chongqing University), Ministry of Education, Chongqing 400045, China.
E-mail address: lipengcheng@cqu.edu.cn (P. Li).

https://doi.org/10.1016/j.jcsr.2018.05.020
0143-974X/

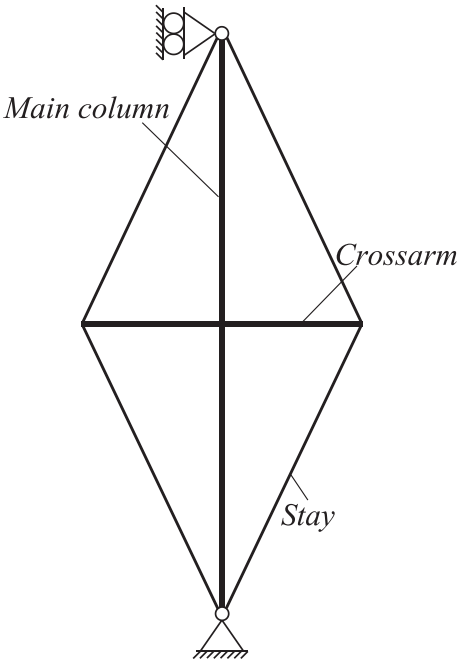

Fig. 1. Composition of PSSC.

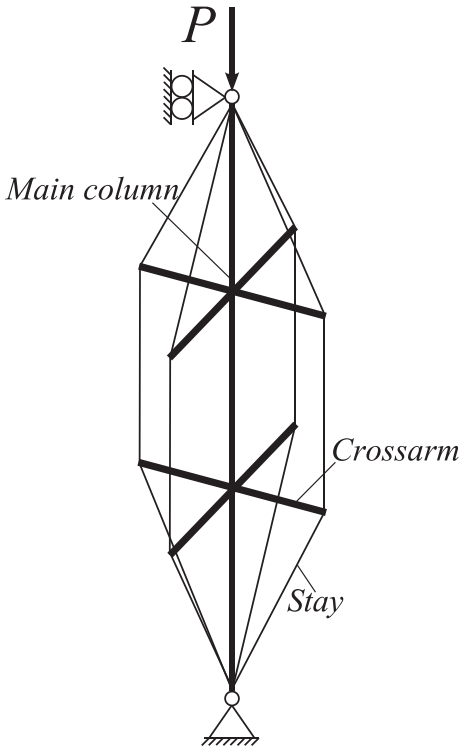

Fig. 3. Structural configuration of PSSCs.

2. Structural configuration and analytical methodology

2.1. Structural configuration

The number of crossarms along the column length can be different in PSSCs with multiple crossarms. As the simplest case of a steel column with multiple crossarms, the current work aims to investigate steel columns stiffened with two-bay crossarms along the column length (see Fig. 3). In this model, all crossarms have equal lengths and are set at the trisection points along the main column. Note that the crosssarms can be pinned or rigidly connected to the main column in practice. However, the pin-connected case is outside the scope of this study. In other words, the connections between the crossarms and main column are thought to be ideally rigid in this work. As for the boundary condition, it is assumed that the column is pin-supported at both ends.

It has been proven that the critical buckling mode is a crucial factor determining the post-buckling behaviour of PSSCs. Thus, the structural parameters, including the crossarm length and stay diameter, should be varied to activate different critical buckling modes in a systematic analysis. To achieve this, a series of different crossarm lengths and stay diameters (see Table 1) was selected in the following FE analysis.

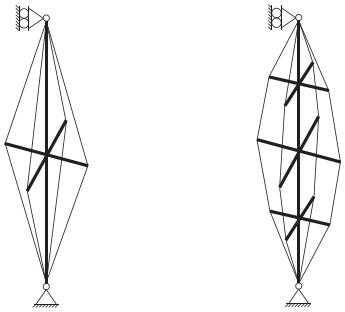

(a) Single-bay stayed column (b) Three-bay stayed column

Fig. 2. Different spatial crossarm layouts along the main column length.

However, it must be noted that the column length was fixed at 5100 mm during the numerical analysis performed in this study. Circular steel tubes with outer and inner diameters of 38.1 mm and 25.4 mm, respectively, were adopted for both the main column and crossarms. Thus, the Young's modulus of the main column and crossarms are 201,000 N/mm^2. Note that the stays in this work are bars, which are the same as those in Hafez's model [2]. Thus, the Young's modulus is assumed to be 202,000 N/mm^2.

2.2. Analytical methodology

As mentioned above, this study focuses on investigating the behaviour of two-bay stayed PSSCs. For the PSSCs stiffened with single-bay crossarms (see Fig. 2(a)), it has been demonstrated that interactive buckling could dominant the buckling strength in some cases. This study would check whether interactive buckling can determine the actual buckling strength for two-bay stayed PSSCs using nonlinear buckling analysis. Note that the initial geometric imperfection must be considered in the nonlinear buckling analysis. Thus, linear buckling analysis should be conducted to obtain the buckling modes, which can be used to construct an imperfect model for nonlinear buckling analysis. It should also be noted that the initial pretension in stays is another crucial factor that can affect the buckling behaviour of PSSCs. To make the numerical analytical results comparable, a benchmark must be defined for the initial pretensions in stays. In this work, pretension corresponds to the maximum critical buckling load is adopted as the benchmark for pretension in stays. Based on these statements, the analytical process in this study can be summarised as follows:

Table 1
Analytical parameters.

Crossarm length (mm)	255	382.5	510	637.5	765
Stay diameter (mm)	1.6	3.2	4.8	6.4	8.0

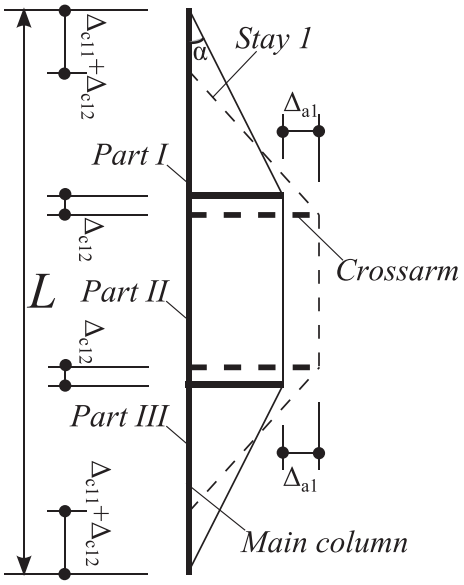

Fig. 4. Deformation of the PSSCs.

(1) Pre-buckling analysis: Pre-buckling analysis was conducted by analysing geometric deformation of the PSSCs in order to derive the mathematical formula used to calculate the initial pretension in stays.
(2) Linear buckling analysis: Linear buckling analysis is based on the un-deformed configuration of the PSSCs and aims to obtain the critical buckling load and the corresponding buckling mode.
(3) Nonlinear buckling analysis: Nonlinear buckling analysis focuses on examining the actual buckling strength of PSSCs and checking whether interactive buckling should be considered when designing this type of column. Moreover, a parametric study has also been conducted by nonlinear buckling analysis to investigate the influencing factors of the buckling strength of PSSCs.

ABAQUS software was selected for numerical analysis in this work, and the arc length method was adopted to obtain the full load-displacement curve used for nonlinear buckling analysis. As for the element type used in linear and nonlinear buckling analyses, shell elements (element type S4R) were selected to simulate both the main column and crossarms, and tension-only truss elements (element type T3D2) were used to model the stays. It should be noted that beam elements have been shown to be appropriate for simulating the column [3,8,11]. However, local buckling cannot be considered based on the beam elements. Based on this consideration, shell elements were adopted to model the column and crossarms, although local buckling has not been observed in the following analyses.

3. Pre-buckling analysis

To establish the relationship between the critical buckling load and pretension in stays by geometric analysis. The following assumptions are made during the derivation:

(1) Displacements are so small that the formulas can be derived based on the un-deformed geometric configuration.
(2) Bending deformations of the crossarms can be ignored.

As shown in Fig. 3, the crossarms are set symmetrically around the main column. Thus, a quarter of this PSSC was taken out as a free-body in this section to perform the derivation (see Fig. 4). Recalling the description of the analytical model for a PSSC in Section 2.1, the

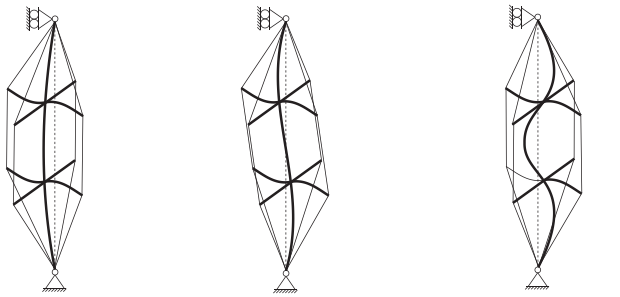

(a)Half sine wave (Mode I) (b)Full sine wave (Mode II) (c)Three half sine wave (Mode III)

Fig. 5. Critical buckling modes for PSSCs.

crossarms are set at the trisection points along the main column length. Thus, the main column can be divided into three parts, which were numbered by “Part I”, “Part II”, and “Part III”, from top to bottom (see Fig. 4). Similarly, the stay which linked the crossarm and the upper end of the column was denoted as “Stay I”. To distinguish deformations of the PSSC under axial compression load, the deformed and un-deformed configurations are depicted by the dotted and solid lines in Fig. 4, respectively.

For small deformations, the length change of stay I Δ_{s1} can be expressed by:

$$\Delta_{s1} = \Delta_{c11}\cos\alpha - \Delta_{a1}\sin\alpha \tag{1}$$

where Δ_{c11} is the end-shortening of Part I, Δ_{a1} is the elongation of the crossarm due to the decrease of the pretension in stays, and α is the angle between the main column and stay I.

The initial axial force P_i in Part I, which results from pretension in the stays, can be calculated by:

$$P_i = 4T_i\cos\alpha \tag{2}$$

in which T_i is the initial pretension in stays.

Similarly, the initial axial force F_i in the crossarm resulting from pretension is:

$$F_i = T_i\sin\alpha \tag{3}$$

The final axial force P_f in Part I after applying the axial compression load P is:

$$P_f = P + 4T_f\cos\alpha \tag{4}$$

where T_f is the final axial force in the stay.

The final axial force in the crossarm after applying an external load P is:

$$F_f = T_f\sin\alpha \tag{5}$$

Considering the initial and final axial forces in Part I (see Eqs. (2) and (4)), the end-shortening of Part I Δ_{c11} can be calculated by:

$$\Delta c_{11} = \frac{P_f - P_i}{K_{c1}} = \frac{P - 4(T_i - T_f)\cos\alpha}{K_{c1}} \tag{6}$$

where K_{c1} is the axial stiffness of Part I, which can be also expressed as the axial stiffness of the main column K_c, as shown in Eq. (7):

$$K_{c1} = 3K_c = \frac{3E_cA_c}{L} \tag{7}$$

where L is the main column length, and E_c and A_c are the Young's modulus and cross-sectional area of the main column, respectively.

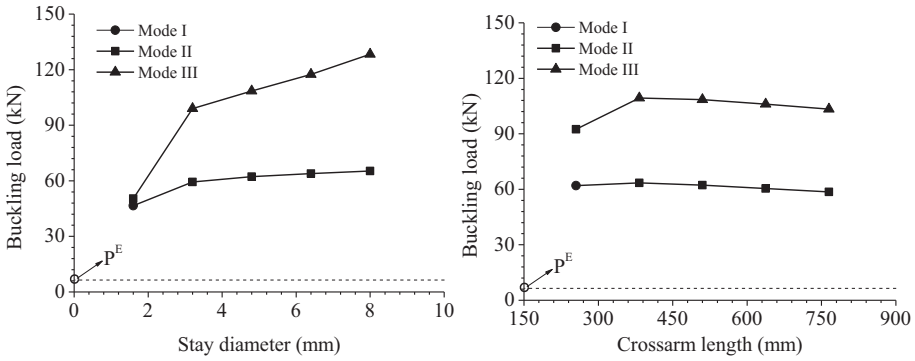

(a) Stay diameter varying (a=510 mm) (b) Crossarm length varying ($\phi_s = 4.8\ mm$)

Fig. 6. Variety of critical buckling loads with different crossarm lengths and stay diameters.

Table 2
Comparison between the capacities obtained from experimental and numerical studies.

Column	Main column (mm)		Crossarm (mm)		Stay dimeter (mm)	Pretension (kN)	$\frac{P_{exp}}{P_{num}}$
	Section	Length	Section	Length			
C08	CHS 139.7 × 6.3	18,000	CHS 101.6 × 8.0	600	10	5.5	0.93
	CHS 139.7 × 6.3	18,000	CHS 101.6 × 8.0	600	13	7.5	0.91
C11	CHS 177.8 × 6.3	18,000	CHS 101.6 × 8.0	600	10	5.5	1.03
	CHS 177.8 × 6.3	18,000	CHS 101.6 × 8.0	600	13	7.5	1.03

Similarly, elongation of the crossarm Δ_a can be expressed by the following:

$$\Delta_{a1} = \frac{F_i - F_f}{K_a} = \frac{(T_i - T_f)\ \sin\alpha}{K_a} \tag{8}$$

where K_a is the axial stiffness of the crossarms.

The shortening of stay I can be expressed by axial forces in the stays, as shown in Eq. (9):

$$\Delta_{s1} = \frac{T_i - T_f}{K_s} \tag{9}$$

where K_s is the stay stiffness.

Substituting Eqs. (6), (8), and (9) into eq. (1), the shortening of stay I can be also expressed by:

$$\Delta_{s1} = \frac{T_i - T_f}{K_s} = \frac{[P - 4(T_i - T_f)\ \cos\alpha]\ \cos\alpha}{K_{c1}} - \frac{[(T_i - T_f)\ \sin\alpha]\ \sin\alpha}{K_a} \tag{10}$$

Thus, the change in axial force in the stay can be obtained by combing Eqs. (9) and (10):

$$T_i - T_f = P\frac{\cos\alpha}{K_{c1}\left(\frac{1}{K_s} + \frac{\sin^2\alpha}{K_a} + \frac{4\ \cos^2\alpha}{K_{c1}}\right)} \tag{11}$$

As for the final axial force in the stay, T_f can be obtained by substituting Eqs. (4), (6), (8), and (9) to eq. (1):

$$T_f = T_i - \frac{(P_f - 4T_i\ \cos\alpha)\ \cos\alpha}{K_{c1}\left(\frac{1}{K_s} + \frac{\sin^2\alpha}{K_a}\right)} \tag{12}$$

Recalling the expression used to calculate P_f in eq. (4), the external load P can be expressed using eq. (13) by combining Eqs. (4) and (12):

$$P = (P_f - 4T_i\ \cos\alpha)\left\{1 + \frac{4\ \cos^2\alpha}{K_{c1}\left(\frac{1}{K_s} + \frac{\sin^2\alpha}{K_a}\right)}\right\} \tag{13}$$

The optimal initial pretension T_{opt} corresponds to the maximum buckling load. Thus, the stays slack at the instant when buckling occurs. By simplifying Eq. (11), the optimal pretension T_{opt} can be expressed by Eq. (14):

$$T_{\text{opt}} = P\frac{\cos\alpha}{K_{c1}\left(\frac{1}{K_s} + \frac{\sin^2\alpha}{K_a} + \frac{4\ \cos^2\alpha}{K_{c1}}\right)} \tag{14}$$

The relationship between P and P_f can be established from eq. (13). Based on this, T_{opt} can be calculated using Eqs. (15) and (16):

$$T_{opt} = CP^c_{T=0} \tag{15}$$

Table 3
Constructed imperfections.

Shape function	Buckling modes	Weight coefficient					
$W_1(x)$	Mode I and Mode II	μ_{11}	0.0000	0.2500	0.5000	0.7500	1.0000
		μ_{12}	0.5000	0.4841	0.4330	0.3307	0.0000
$W_2(x)$	Mode II and Mode III	μ_{22}	0.0000	0.1250	0.2500	0.3750	0.5000
		μ_{23}	0.3333	0.3227	0.2887	0.2205	0.0000

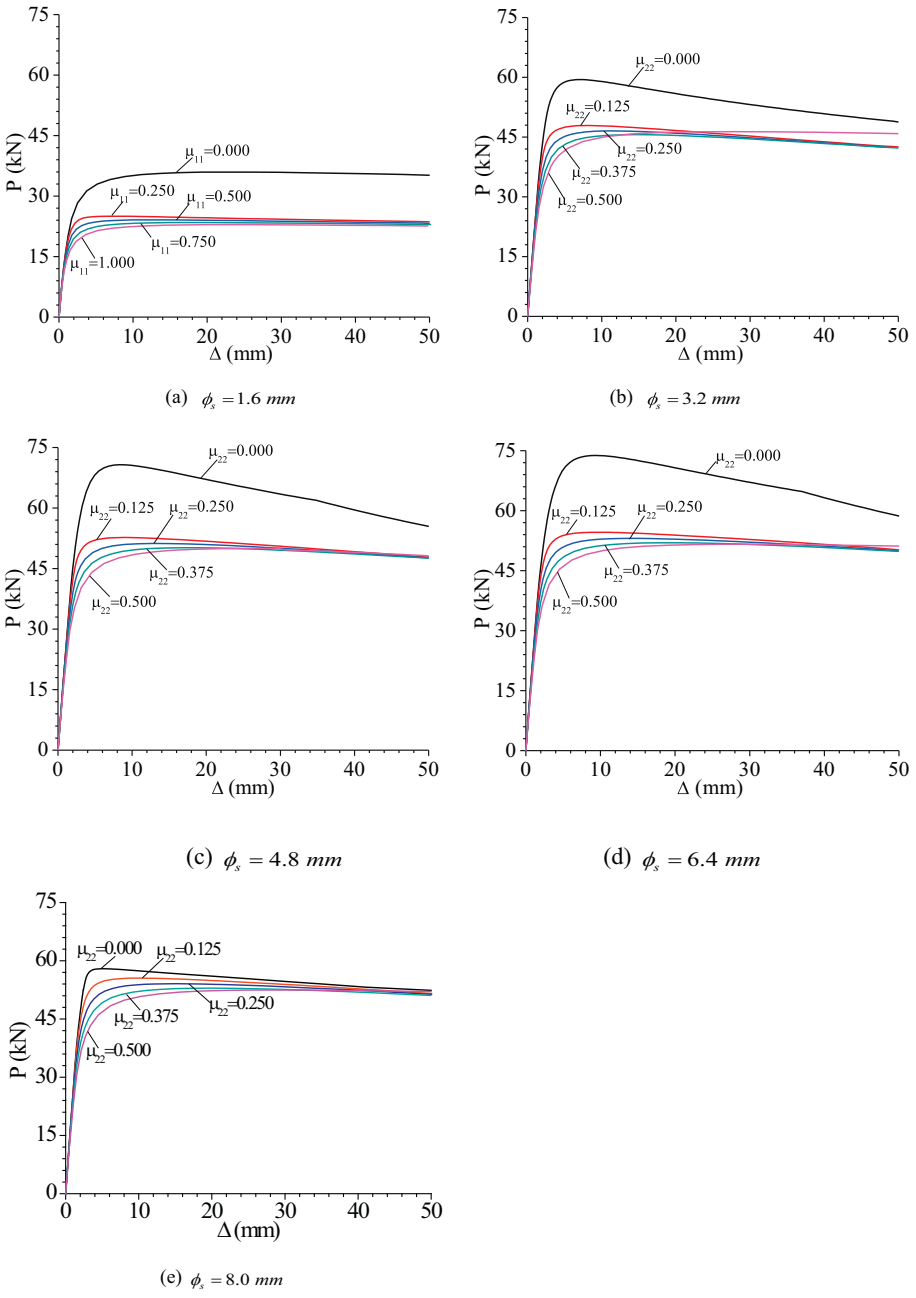

Fig. 7. Axial load to end-shortening curves (a = 510 mm).

$$C = \frac{\left(\frac{1}{K_s} + \frac{\sin^2\alpha}{K_a}\right)\cos\alpha}{\left(\frac{1}{K_s} + \frac{\sin^2\alpha}{K_a} + \frac{4\cos^2\alpha}{K_{c1}}\right)\left(K_{c1}\left(\frac{1}{K_s} + \frac{\sin^2\alpha}{K_a}\right) + 4\cos^2\alpha\right)} \tag{16}$$

where $P^c_{T=0}$ is the buckling load calculated from FE analysis when the initial pretension is zero.

4. Linear buckling analysis

For a PSSC with single-bay crossarm, it has been shown that the critical buckling modes of the main column are approximately a half sine wave and full sine wave. However, whether these critical buckling modes can be changed by the two-bay crossarm is unknown. Thus, investigating the buckling modes is the primary focus of this section. Apart from the buckling mode, the critical buckling load is another focus of this section. To make the analytical results more convincing, PSSCs with different crossarm lengths and stay diameters shown in Table 1 were analysed. According to the linear buckling analysis, it has been found that the critical buckling modes of the two-bay stayed PSSCs can be approximately taken as half sine wave, full sine wave, and three half sine waves, as depicted in Fig. 5. In other words, the critical buckling mode becomes more complicated for PSSCs with two-bay crossarms. For convenience, these three buckling modes are named "Mode I", "Mode II", and "Mode III", respectively.

Fig. 6 shows the various critical buckling loads in a PSSC with different crossarm lengths and stay diameters. Note that the lowest mode Euler load on the main column P^E has also been indicated in Fig. 6 to illustrate the effect of pre-tensioned stays on the buckling load in the PSSC. Obviously, the buckling load on the main column P^E can be

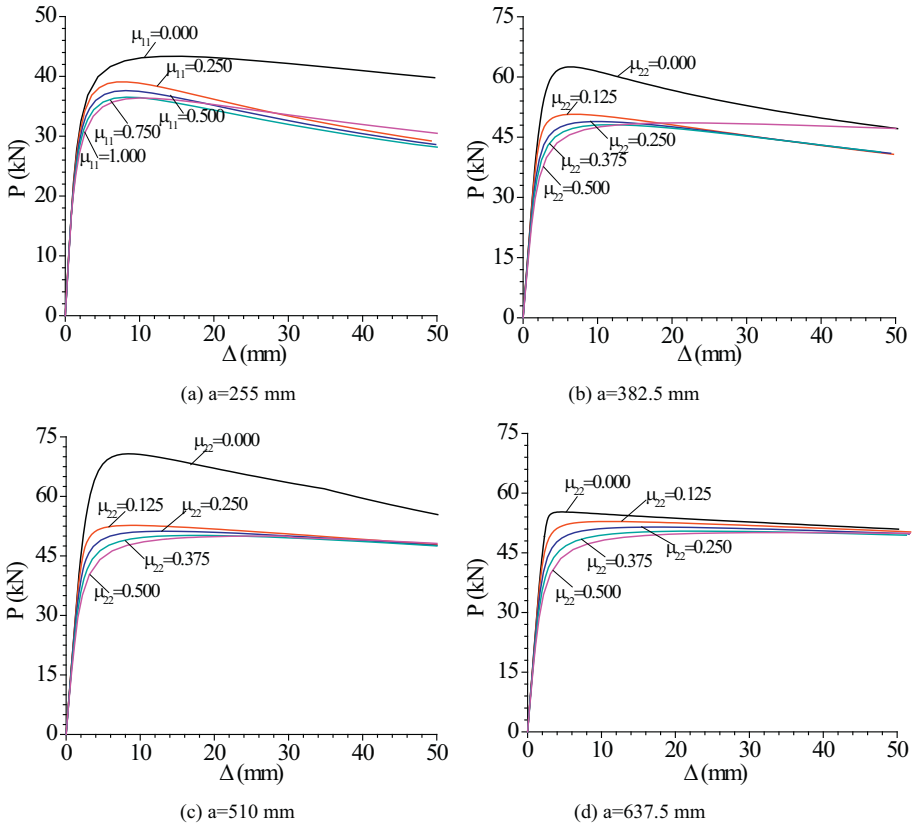

Fig. 8. Axial load to end-shortening curves ($\phi_s = 4.8mm$).

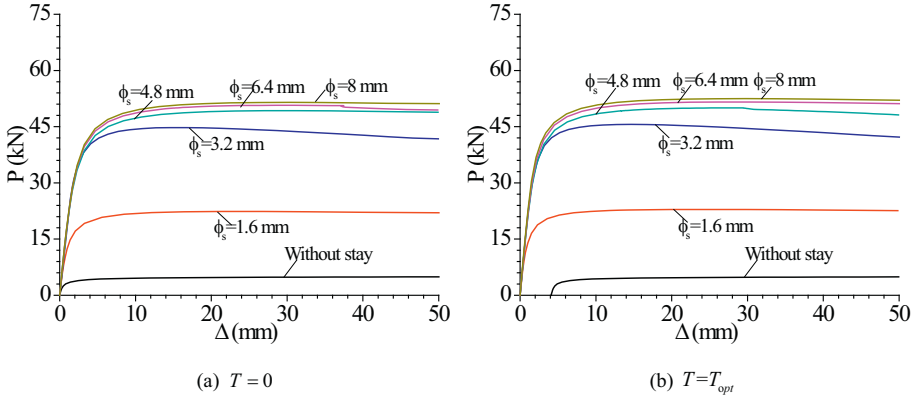

Fig. 9. Axial load to end-shortening curves with different stay diameters (a = 510 mm).

significantly improved by using pre-tensioned stays. When the stay diameter is 4.8 mm, the lowest buckling load on the PSSC could reach around 10 times the value of P^E.

5. Nonlinear buckling analysis

5.1. Validation of the numerical analysis

In order to validate the accuracy of the numerical buckling analysis, experimental buckling results for the two-bay PSSCs denoted "C08" and "C11" in reference [16] were selected for verification. Note that the nominal length of these PSSCs was 18,000 mm, and the main column and crossarms were fabricated from S355 steel and S690 steel, respectively. More details regarding the PSSCs are presented in Table 2. In Table 2, the symbols P_{exp} and P_{num} represent the load capacities obtained from experimental and numerical analyses, respectively. Obviously, the maximum difference between the experimental and numerical results is less than 10%, implying that buckling analysis is accurate enough to estimate the load carrying capacities of PSSCs.

5.2. Imperfection construction

Having validated the accuracy of the numerical analysis, it is essential to carry out nonlinear buckling analysis to investigate the post

Table 4
Initial pretension T_{opt} with stay diameter varying (a = 510 mm).

Stay diameter (mm)	1.6	3.2	4.8	6.4	8.0
T_{opt} (MPa)	66.368	79.223	74.754	66.886	57.947

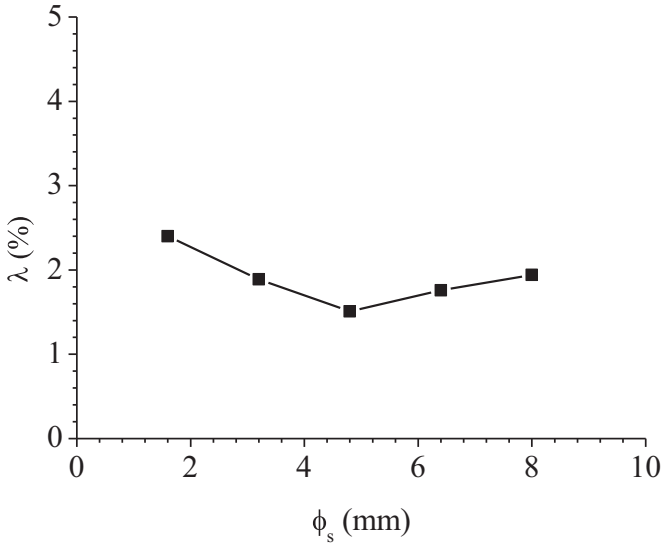

Fig. 10. Comparison between the axial loads when $T = 0$ and $T = T_{opt}$.

buckling behaviour of PSSCs. However, it should also be noted that geometric imperfection is one of the most important factors that can affect the stability of steel columns. Thus, geometric imperfection must be taken into account in a nonlinear buckling analysis [17,18]. For PSSCs with single-bay crossarms (see Fig. 2(a)), interactive buckling may become the dominant case for determining the actual buckling strength [3]. Considering the effect of interactive buckling, an asymmetric geometric imperfection distribution was established by combining different critical buckling modes. Unfortunately, the analysis in Section 4 shows that the critical buckling modes in two-bay stayed PSSCs are different from those of single-bay PSSCs. This situation makes it impossible to directly adopt the aforementioned method to analyse the two-bay PSSCs in this study. Therefore, it is essential to reconstruct geometric imperfections to examine whether interactive buckling could become the dominant case by determining the actual load carrying capacities of PSSCs. This issue would be resolved by extending the method in [3].

As shown in Fig. 5, the critical buckling modes of two-bay PSSCs can be Mode I, Mode II, and Mode III. There are two possible combinations for the first two buckling mode shapes, i.e. Mode I and Mode II, or Mode II and Mode III. In this study, the first two buckling mode shapes were adopted to construct a new geometric imperfection for use in nonlinear buckling analysis. Thus, two different functions $W_1(x)$ and $W_2(x)$ (see Eqs. (17) and (18), respectively) were established to describe

Table 5
Crossarm lengths corresponding to the maximum load carrying capacities.

Stay diameters (mm)		1.6	3.2	4.8	6.4	8.0
Crossarm lengths (mm)	$T = 0$	765	765	637.5	510	510
	$T = T_{opt}$	765	765	637.5	510	510

the two-mode combinations.

$$W_1(x) = \Delta_w \left[\mu_{11} \sin\frac{\pi x}{L} + \mu_{12} \sin\frac{2\pi x}{L}\right] \tag{17}$$

$$W_2(x) = \Delta_w \left[\mu_{22} \sin\frac{2\pi x}{L} + \mu_{23} \sin\frac{3\pi x}{L}\right] \tag{18}$$

In the above equations, Δ_w is the maximum magnitude of the constructed imperfection, and μ_{11}, μ_{12}, μ_{22}, and μ_{23} are coefficients, which will be explained in the next paragraph.

The first and second terms on the right side of Eq. (17) are adopted to simulate the buckling shapes of Mode I and Mode II, respectively. Therefore, μ_{11} and μ_{12} can be taken as weight coefficients for Mode I and Mode II in the shape function $W_1(x)$, respectively. Similarly, μ_{22} and μ_{23} are the weight coefficients of Mode II and Mode III in the shape function $W_2(x)$, respectively. In other words, the imperfection shape of $W_1(x)$ or $W_2(x)$ is constructed from Mode I and Mode II or Mode II and Mode III with different weight coefficients. Thus, the values of μ_{11}, μ_{12}, μ_{22}, and μ_{23} must be determined in order to define the imperfection shapes. In this work, it is assumed that shortening is the same in all main columns, regardless of whether bending follows purely Mode I or the constructed imperfection shapes. Based on this assumption, the relationships between μ_{11} and μ_{12}, or μ_{22} and μ_{23} can be expressed using eqs. (19) and (20), respectively:

$$\mu_{11}^2 + 4\mu_{12}^2 = 1 \tag{19}$$

$$4\mu_{22}^2 + 9\mu_{23}^2 = 1 \tag{20}$$

Typical values of μ_{11} and μ_{12}, or μ_{22} and μ_{23} were selected in the following numerical analyses (see Table 3). According to the geometric construction method stated above, one can conclude that different weight coefficient values intrinsically correspond to different imperfection shapes.

Except for the imperfection shape, the imperfection magnitude is also an important factor affecting the stability of PSSCs. In this study, the imperfection magnitude is assumed to be L/300 (L is the main column length) in numerical analysis.

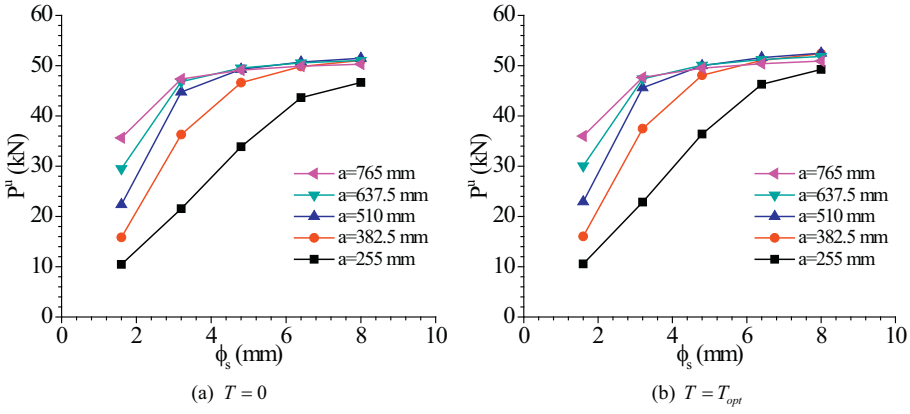

Fig. 11. Load carrying capacities of PSSCs with different crossarm length and varying stay diameter.

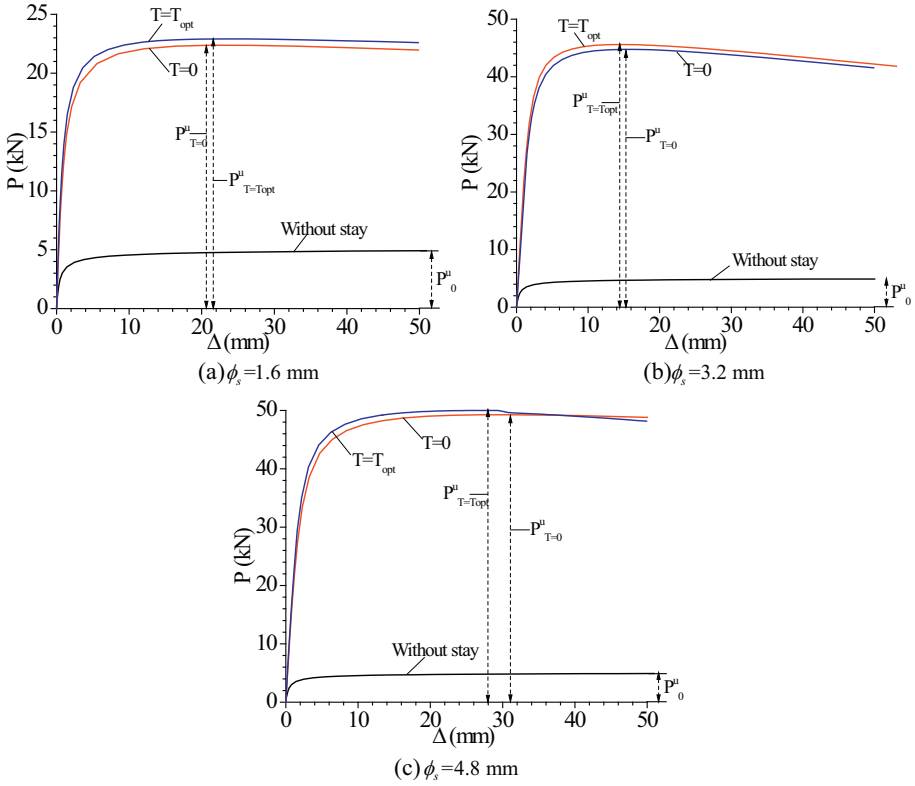

Fig. 12. Axial load to end-shortening curves of PSSCs (a = 510 mm).

5.3. Post-buckling analysis

Having constructed the geometric imperfections in Section 5.2, nonlinear buckling analysis can be conducted by adopting different geometric imperfections to examine whether interactive buckling could dominate in regards to the actual buckling load. In this section, it is worth noting that the imperfection shape $W_1(x)$ is adopted when the shapes of the first two buckling modes are Mode I and Mode II. In contrast, the imperfection shape $W_2(x)$ is introduced when the shapes of the first two buckling modes are Mode II and Mode III. Thus, linear buckling analysis must be conducted prior to nonlinear buckling analysis in order to determine the appropriate imperfection shape. Figs. 7 and 8 present nonlinear buckling analysis results, which are represented by the axial load to end-shortening curves with different stay diameters and crossarm lengths. For the analyses in this section, the pretension in stays is assumed to be T_{opt}. Comparing Figs. 6, 7, and 8, it is interesting to note that the imperfection corresponding to the actual buckling load is generally determined by distinct buckling modes, with the exceptions of Figs. 7(b) and 8(b). As shown in Figs. 7(b) and 8(b), the load carrying capacities correspond to $\mu_{22} = 0.375$ are slightly lower than those corresponding to the distinct buckling mode ($\mu_{22} = 0.500$). This implies that the actual load carrying capacity of a PSSC is determined by interactive buckling. However, it should also be noted that discrepancies between the load carrying capacities corresponding to $\mu_{22} = 0.375$ and $\mu_{22} = 0.500$ are negligible in these two cases. Thus, one can conclude that the effect of interactive buckling on the load-carrying capacities of two-bay PSSCs can be ignored, i.e., the geometric imperfection following the lowest buckling mode can be used to determine the buckling strength using nonlinear buckling analysis. This is the most notable difference between single-bay and two-bay PSSCs when selecting the initial geometric imperfections used in nonlinear buckling analysis.

5.4. Discussion

Linear and nonlinear buckling analysis of the two-bay PSSCs were conducted in the above sections. This section aims to discuss how pretension in stays and stay diameter affect the buckling strength of PSSCs. In this section, the imposed geometric imperfection follows the distinct buckling mode in the nonlinear buckling analysis. In other words, interactive buckling is ignored when introducing imperfections.

5.4.1. Effect of stay diameter

The load carrying capacities are enhanced by the pre-tensioned stays. Thus, buckling could certainly be affected by the stay diameters. To investigate the effect of stay diameters, nonlinear buckling analysis was conducted in this section. Fig. 9 shows the axial load to end-shortening curves with different stay diameters when $T = 0$ and $T = T_{opt}$. Recalling Eqs. (15) and (16), the pretension T_{opt} corresponding to the parameters shown in Fig. 9 can be calculated (see Table 4).

In order to investigate the effect of stay diameter, the load to end-shortening curve of an ordinary un-stiffened column has also been shown in Fig. 9. Obviously, the load carrying capacity of the steel column can be significantly enhanced by increasing the stay diameter, especially when the stay diameter is less than 4.8 mm. Recalling the critical buckling mode shown in Fig. 6, it is interesting to note that the critical buckling mode is Mode II when the stay diameter is larger than 3.2 mm. Thus, it can be concluded that increasing the stay diameter could effectively improve the load carrying capacity of a PSSC when the critical buckling mode is Mode I. However, increasing the stay diameter becomes less effective when the critical buckling mode is Mode II.

It should be noted that the differences between Figs. 9(a) and 9(b) are quite minor. To discuss the differences between these two figures,

a parameter λ defined in eq. (21) is introduced:

$$\lambda = \frac{P_{T=T\text{opt}} - P_{T=0}}{P_{T=0}} \tag{21}$$

$P_{T=T\text{opt}}$ and $P_{T=0}$ are the nonlinear buckling loads when $T = T_{opt}$ and $T = 0$, respectively. Fig. 10 shows the relationship between λ and ϕ_s when the crossarm length is 510 mm. Obviously, the load carrying capacity can be improved by approximately 2% when the initial pretension is increased from $T = 0$ to $T = T_{opt}$. More details regarding the effect of pretension in stays will be discussed in the next section.

Fig. 11 summarises the load carrying capacities of PSSCs with crossarm length varying from 255 mm to 765 mm when the pretension is zero and T_{opt}. Similar results to Fig. 9 can be observed, and the load carrying capacities are generally improved with increased stay diameter. However, it should also be noted that the load carrying capacity can be decreased by increasing the crossarm length when the stay diameter is large, because the axial stiffness becomes much smaller when the crossarm length is increasing.

Table 5 shows the crossarm lengths corresponding to the maximum load carrying capacities when the stay diameters are fixed. When the stay diameter is 1.6 mm or 3.2 mm, the maximum load carrying capacities correspond to the maximum crossarm length (765 mm). In other words, the capacity can always be increased by increasing the crossarm length in these two cases. However, when the stay diameter is larger than 3.2 mm, the maximum capacity does not correspond to the maximum crossarm length. Thus, one can conclude that the effect of crossarm length on load capacity becomes adverse when the stay diameter is large.

5.4.2. Effect of pretension in stays

The effect of stay diameter on the stability of PSSCs was discussed in the above section. However, whether stay diameter and pretension have the same contributions to improved buckling strength is unknown and should be studied. This issue could be resolved by conducting nonlinear buckling analysis on PSSCs with $T = 0$ and $T = T_{opt}$. Similarly, the un-stiffened ordinary column has also been studied for comparison. Fig. 12 presents the axial load-to-end shortening curves of PSSCs with different stay diameters when the crossarm length is 510 mm. In Fig. 12, the load carrying capacity of an ordinary steel column is denoted by P_0^u, and the capacities of PSSCs with pretension $T = 0$ and $T = T_{opt}$ are represented by $P_{T=0}^u$ and $P_{T=Topt}^u$, respectively. Thus, the effect of stay and pretension in stays can be respectively obtained by comparing P_0^u, $P_{T=0}^u$ and $P_{T=0}^u$, $P_{T=Topt}^u$. Obviously, the load carrying capacity of an ordinary steel column can be significantly enhanced by the stay even though the pretension in stays is zero, because the stay stiffness can be activated automatically due to column deformation.

6. Conclusions

The stability behaviour of the two-bay prestressed stayed steel column was geometrically and numerically investigated in this study. Both linear and nonlinear buckling analyses were performed. The influence of the crossarm length and pretension in the stays were studied. Conclusions drawn from this study are as follows:

(1) According to the geometric analysis, it has been demonstrated that the relationship between pretension in stays and the linear buckling load can be described by a single equation. Moreover, the equation used to determine pretension in stays which corresponds to the maximum buckling load has been proposed.
(2) The critical buckling modes of two-bay PSSCs are more complicated than the single-bay PSSCs. The critical buckling mode in this structure can be observed to have a shape that is similar of three halves of a sine curve. However, this buckling mode cannot be observed as the lowest buckling mode in single-bay PSSCs.
(3) Based on the nonlinear buckling analysis results, it has been found that the effect of interactive buckling can be ignored when determining the actual buckling load of two-bay PSSCs. In other words, it is safe enough to introduce geometric imperfections following the lowest buckling mode when designing this structure. In contrast, an asymmetric imperfection must be constructed to determine the actual buckling strength of single-bay PSSCs in some cases.
(4) The effects of stay diameter and pretension in stays on the buckling strength of PSSCs have been investigated. It has been found that a stay without pretension can effectively improve the load-carrying capacity of ordinary steel columns, because the stay stiffness can be automatically activated by deformation of the steel column. Thus, the effect is limited when adopting high pretensions to increase the buckling strength of PSSCs.

Acknowledgement

The authors gratefully acknowledge the support provided by the Fundamental Research Funds for the Central Universities (No. 106112017CDJXY200008 and No. 106112016CDJRC000088).

References

[1] K. Chu, S.S. Berge, Analysis and design of struts with tension ties [J], J. Struct. Div. 89 (1) (1963) 127–163.
[2] H.H. Hafez, M.C. Temple, J.S. Ellis, Pre-tensioning of single-crossarm stayed columns [J], J. Struct. Div. 105 (2) (1979) 359–375.
[3] D. Saito, M.A. Wadee, Numerical studies of interactive buckling in prestressed steel stayed columns [J], Eng. Struct. 31 (2) (2009) 432–443.
[4] P.C. Li, M.A. Wadee, J.L. Yu, N.G. Christie, M.E. Wu, Stability of prestressed stayed steel columns with a three branch crossarm system [J], J. Constr. Steel Res. 122 (2016) 274–291.
[5] C. Dou, Y.L. Pi, Effects of geometric imperfections on flexural buckling resistance of laterally braced columns, J. Struct. Eng. 142 (9) (2016), 04016048.
[6] D. Saito, M.A. Wadee, Post-buckling behaviour of prestressed steel stayed columns [J], Eng. Struct. 30 (5) (2008) 1224–1239.
[7] S.L. Chan, G.P. Shu, Z.T. Lv, Stability analysis and parametric study of pre-stressed stayed columns [J], Eng. Struct. 24 (2002) 115–124.
[8] D. Saito, M.A. Wadee, Optimal prestressing and configuration of stayed columns, Proceedings of the ICE - Structures and Buildings, Vol. 163(5), 2010, pp. 343–355.
[9] J.V. Steirteghem, W.P. De Wilde, P. Samyn, B.P. Verbeeck, F. Wattel, Optimum design of stayed columns with split-up cross arm [J], Adv. Eng. Softw. 36 (2005) 614–625.
[10] M.E. Wu, M. Sasaki, H. Ohmori, Geometrically nonlinear analysis and experiment on pin joint stayed column, Proceedings of IASS (2002) 233–240.
[11] A.I. Osofero, M.A. Wadee, L. Gardner, Experimental study of critical and post-buckling behaviour of prestressed stayed column, J. Constr. Res. 79 (2012) 226–241.
[12] R.R. De Araujo, S.A.L. de Andrade, P.C.G. da S Vellasco, J.G.S. da Silva, L.R.O. de Lima, Experimental and numerical assessment of stayed steel columns, J. Constr. Steel Res. 64 (2008) 1020–1029.
[13] M. Serra, A. Shahbazian, L. da S Simões, L. Marques, C. Rebelo, P.C.G. da S Vellasco, A full scale experimental study of prestressed stayed columns, Eng. Struct. 10 (2015) 490–510.
[14] G.P. Shu, S.M. Hou, D.H. Chen, H.Y. Bao, J. Gu, Experimental research on prestressed stayed columns with inner brace [J], Journal of Building Structures 27 (5) (2006) 79–117 (in Chinese).
[15] L. Lapira, M.A. Wadee, L. Gardner, Stability of multiple-crossarm prestressed stayed columns with additional stay systems [J], Structure 12 (2017) 227–241.
[16] J.P. Martins, A. Shahbazian, L.S. da Silva, C. Rebelo, R. Simões, Structural behaviour of prestressed stayed columns with single and double cross-arms using normal and high strength steel [J], Archives of Civil and Mechanical Engineering 16 (2016) 618–633.
[17] A.M.G. Coelho, P.D. Simão, M.A. Wadee, Imperfection sensitivity of column instability revisited [J], J. Constr. Steel Res. 90 (2013) 265–282.
[18] J.D. Aristizabal-Ochoa, Stability of imperfect columns with nonlinear connections under eccentric axial loads including shear effects [J], Int. J. Mech. Sci. 90 (2015) 61–76.